S100A9 and HMGB1 orchestrate MDSC-mediated immunosuppression in melanoma through TLR4 signaling

Feyza Gül Özbay Kurt [1,2,3,4] Beatrice-Ana Cicortas,[1,2,3,4] Bianca M Balzasch,[5] Carolina De la Torre,[6] Volker Ast,[6] Ece Tavukcuoglu,[1,2] Cagla Ak,[1,2,3,4] Sebastian A Wohlfeil,[1,2] Adelheid Cerwenka,[5] Jochen Utikal,[1,2,3,4] Viktor Umansky [1,2,3,4]

ABSTRACT

Background Immunotherapies for malignant melanoma are challenged by the resistance developed in a significant proportion of patients. Myeloid-derived suppressor cells (MDSC), with their ability to inhibit antitumor T-cell responses, are a major contributor to immunosuppression and resistance to immune checkpoint therapies in melanoma. Damage-associated molecular patterns S100A8, S100A9, and HMGB1, acting as toll like receptor 4 (TLR4) and receptor for advanced glycation endproducts (RAGE) ligands, are highly expressed in the tumor microenvironment and drive MDSC activation. However, the role of TLR4 and RAGE signaling in the acquisition of MDSC immunosuppressive properties remains to be better defined. Our study investigates how the signaling via TLR4 and RAGE as well as their ligands S100A9 and HMGB1, shape MDSC-mediated immunosuppression in melanoma.

Methods MDSC were isolated from the peripheral blood of patients with advanced melanoma or generated in vitro from healthy donor-derived monocytes. Monocytes were treated with S100A9 or HMGB1 for 72 hours. The immunosuppressive capacity of treated monocytes was assessed in the inhibition of T-cell proliferation assay in the presence or absence of TLR4 and RAGE inhibitors. Plasma levels of S100A8/9 and HMGB1 were quantified by ELISA. Single-cell RNA sequencing (scRNA-seq) was performed on monocytes from patients with melanoma and healthy donors.

Results We showed that exposure to S100A9 and HMGB1 converted healthy donor-derived monocytes into MDSC through TLR4 signaling. Our scRNA-seq data revealed in patient monocytes enriched inflammatory genes, including *S100* and those involved in NF-κB and TLR4 signaling, and a reduced major histocompatibility complex II gene expression. Furthermore, elevated plasma S100A8/9 levels correlated with shorter progression-free survival in patients with melanoma.

Conclusions These findings highlight the critical role of TLR4 and, to a lesser extent, RAGE signaling in the conversion of monocytes into MDSC-like cells, underscore the potential of targeting S100A9 to prevent this conversion, and highlight the prognostic value of S100A8/9 as a plasma biomarker in melanoma.

WHAT IS ALREADY KNOWN ON THIS TOPIC

⇒ Immunotherapies, particularly immune checkpoint inhibitors (ICI), have been pivotal in treating malignant melanoma yet face challenges due to the development of resistance in a significant subset of patients. Myeloid-derived suppressor cells (MDSC) are recognized for their role in promoting immunosuppression within the tumor microenvironment, impairing antitumor T-cell responses and contributing to resistance against immunotherapies. Damage-associated molecular patterns such as S100A8, S100A9, and HMGB1, interacting with receptors toll like receptor 4 (TLR4) and receptor for advanced glycation endproducts, are implicated in cancer progression, including activating MDSC within tumors.

WHAT THIS STUDY ADDS

⇒ This research primarily elucidated the role of S100A9 in converting monocytes into immunosuppressive MDSC through the TLR4 pathway. Single-cell RNA sequencing of monocytes from patients with melanoma revealed elevated expression of S100 genes and genes involved in NF-κB and TLR4 signaling as well as reduced expression of major histocompatibility complex II genes. Furthermore, the association between high plasma levels of S100A8/9 and shorter progression-free survival in patients with melanoma suggests these molecules as potential prognostic biomarkers for monitoring disease progression and response to ICI therapy.

HOW THIS STUDY MIGHT AFFECT RESEARCH, PRACTICE OR POLICY

⇒ The findings suggest new research directions focusing on the targeting of TLR4 signaling pathways to mitigate MDSC-mediated immunosuppression in melanoma. S100A8/9 could serve as a potential biomarker for monitoring disease progression and therapeutic response, potentially influencing future treatment guidelines to improve the efficacy of ICI.

BACKGROUND

Despite its increased immunogenicity, malignant melanoma is characterized by a strong immunosuppression, in which

myeloid-derived suppressor cells (MDSC) play a pivotal role.[1] MDSC represent a heterogenous population of myeloid cells with immunosuppressive functions that are known to be enriched in circulation and in the tumor microenvironment (TME).[2] The level of circulating MDSC was reported to be associated with high tumor burden and poor response to immune checkpoint inhibitors (ICI).[3]

In humans, MDSC are categorized into two major subsets: polymorphonuclear (PMN-MDSC) defined as $CD15^+$ $CD33^+HLA-DR^{-/low}$ and mononuclear (M-MDSC) as $CD14^+$ $CD33^+HLA-DR^{-/low}$ cells.[4] MDSC inhibit antitumor immune responses by blocking T and natural killer cell functions via different mechanisms.[5] They express programmed death-ligand 1 (PD-L1) and produce high levels of reactive oxygen species (ROS) and nitric oxide (NO), inducing T-cell anergy.[6] Moreover, they deplete L-arginine and L-tryptophan required for T-cell functions through the activation of arginase-1 (ARG-1), inducible nitric oxide synthase and indoleamine 2,3-dioxygenase 1 (IDO).[7] MDSC also secrete high amounts of transforming growth factor-β and interleukin (IL)-10, thereby inducing regulatory T-cell expansion.[8] Collectively, they create a highly immunosuppressive TME.[9]

Chronic inflammation has been reported to be associated with the onset and progression of melanoma.[10] Long-term secretion of various inflammatory mediators by melanoma and host cells leads to the accumulation and activation of MDSC, as well as the conversion of normal myeloid cells into immunosuppressive MDSC.[11 12] Toll like receptor (TLR) agonists and damage-associated molecular patterns (DAMPs) such as high mobility group box 1 (HMGB1) and S100 calcium-binding proteins can contribute to MDSC generation.[13 14] Increased levels of calprotectin A and B (S100A8 and S100A9) were reported in cancer and shown to be positively correlated with tumor progression and metastasis.[15 16] These proteins are primarily found as heterodimers of S100A8/9 but can also form homodimers and tetramers.[17]

Monocytes and neutrophils release S100A8/9 on stimulation with pro-inflammatory cytokines such as tumor necrosis factor (TNF)-α.[18] Moreover, neutrophils, immature macrophages, MDSC, and tumor cells were demonstrated to express S100A8 and S100A9.[15] HMGB1, a non-histone protein, plays diverse roles in DNA repair, neural development, extracellular signaling, and transcription.[19] Acting as a DAMP and alarmin, it is passively released during necrotic cell death or actively secreted through exocytosis and translocation.[20] An increased level of HMGB1 was shown to be associated with poor prognosis and shorter survival of patients with cancer.[21] Both S100A8/9 and HMGB1 bind either to TLR4 or the receptor for advanced glycation endproducts (RAGE), initiating a complex signaling pathway resulting in the generation of ROS, NO and pro-inflammatory cytokines IL-6, IL-1β, and TNF-α.[22] In addition to TLR4 and RAGE, S100A8/9 can bind to other receptors such as extracellular matrix metalloproteinase inducer, melanoma

cell adhesion molecule, activated leukocyte cell adhesion molecule, and neuroplastin.[23] The involvement of S100A8/9 and HMGB1 in tumor progression has been reported, along with their regulatory role in the enrichment of MDSC.[22 24] However, it remains unclear whether they act mainly through TLR4 or RAGE.[22]

Understanding the factors and signaling pathways involved in MDSC activation and recruitment is pivotal for developing immunotherapeutic strategies targeting MDSC.[25] Here, we demonstrate that S100A9 and HMGB1-treated healthy donor-derived monocytes acquired suppressive activity against T cells associated with increased ROS production, and expression of PD-L1 and IDO-1. Blocking TLR4 signaling with the TLR4 inhibitor resatorvid attenuated the inhibition of T-cell proliferation, indicating that this pathway is mainly involved in S100A9 and HMGB1-induced MDSC generation. Furthermore, single-cell RNA sequencing (scRNA-seq) of $CD14^+$ monocytes from patients with melanoma revealed increased expression of S100 and NF-κB target genes and decreased expression of genes involved in the antigen presentation capacity, including major histocompatibility complex (MHC) class II genes. Finally, we demonstrate that patients with melanoma with high plasma levels of S100A8/9 had increased PD-L1 expression on MDSC and poor progression-free survival (PFS) after ICI therapy.

METHODS
Human sample collection
Patients with stage III-IV melanoma (n=42) who did not receive any therapy for at least 3 months were enrolled after obtaining written informed consent. Patients received ICI such as nivolumab or pembrolizumab alone or nivolumab combined with ipilimumab at the Skin Cancer Center (University Medical Center Mannheim, Germany). 31 patients (73%) received ICI therapy as the first line of treatment, 7 patients (17%) as the second line, and 4 patients (10%) as the third line. The characteristics of patients are displayed in table 1. Peripheral blood samples were collected before (baseline) and 1 month after ICI administration (on-treatment). The response to treatment was evaluated using contrast-enhanced CT, MRI, or positron emission tomography-CT every 12 weeks after the initial ICI administration. Patients were categorized as responders or non-responders based on the immunotherapy Response Evaluation Criteria in Solid Tumors, considering the complete response, partial response, and stable disease as a therapy response and progressive disease as non-response.

Plasma samples were prepared from the peripheral blood of patients with melanoma (n=40). Peripheral blood mononuclear cells (PBMC) were either isolated from patients with melanoma (n=33) or buffy coats obtained from healthy donors (n=86) via density gradient centrifugation using Pancoll (1.077 g/mL, PanBiotech). $CD14^+$ monocytes (n=2; patients with melanoma, n=52, healthy donors) and $CD3^+$ T cells (n=6; patients with

Table 1 Clinical characteristics of patients with melanoma

Characteristics	n=42
Gender, n (%)	
Male	20 (48)
Female	22 (53)
Age, n (%)	
≤65 years	25(60)
≥65 years	17(40)
AJCC stage, n (%)	
IIIB	4 (10)
IIIC	7 (17)
IIID	1 (2)
IV	30 (71)
Treatment line, n (%)	
1	31 (73)
2	7 (17)
3	4 (10)
Therapy, n (%)	
Anti-PD-1	23 (55)
Anti-PD-1/CTLA-4	19 (45)
Progression, n (%)	
Progress	22 (52)
No progress	20 (48)

AJCC, American Joint Committee on Cancer; CTLA-4, cytotoxic T-lymphocyte associated protein 4; PD-1, programmed cell death protein-1 .

melanoma, n=34; healthy donors) were isolated from PBMC by MACS (Miltenyi Biotec) according to the manufacturer's instructions. Plasma samples were separated from the whole blood of patients with melanoma by centrifugation and stored at −80°C until further use.

Isolation and treatment of CD14⁺ monocytes

CD14⁺ monocytes were isolated from healthy and patient-derived PBMCs by MACS (Miltenyi Biotec) according to the manufacturer's instructions. Healthy donor monocytes were subjected to various treatment conditions including inhibitors resatorvid (TAK-242; catalog 243984-11-4, Sigma Aldrich) and FPS-ZM1 (catalog 553030, Sigma Aldrich). Resatorvid is a small molecule inhibitor that specifically blocks TLR4 signaling.[26] FPS-ZM1 acts as an RAGE antagonist, inhibiting interactions with RAGE ligands by binding to this receptor.[27] Monocytes were pretreated with either resatorvid (5 µM) or FPS-ZM1 (30 nm) or DMSO (served as a control) for 1 hour, and were further incubated either with recombinant (r)HMGB1 (5 µg/mL; catalog ab167718, Abcam) or rS100A9 (5 µg/mL; catalog ab287938, Abcam) in the presence of GM-CSF (40 ng/mL; catalog 130-093-865; Miltenyi Biotec) for 72 hours. Monocytes cultured with granulocyte-macrophage colony-stimulating factor (GM-CSF) alone were used as a

control. For the in vitro generation of MDSC, monocytes were treated with GM-CSF (50 ng/mL) and IL-6 (50 ng/mL; catalog 130-093-931, Miltenyi Biotec) for 96 hours.

Flow cytometry

Cells were treated with FcR Blocking Reagent (Miltenyi Biotec) for 15 min at 4°C. Then they were stained with the following monoclonal antibodies (mAbs) and reagents for 30 min at 4°C: Fixable viability dye 700 (1:1,000; catalog 564997, BD Biosciences), anti-human CD14-FITC (1:25; clone MΦP9; catalog 347493, BD Biosciences), PD-L1-BV421 (1:100; clone MIH1; catalog 563738, BD Biosciences), isotype IgG1 BV421 (1:200; catalog 659453, BD), HLA-DR-V500 (1:100; clone G46-6, BD Biosciences), CD33-PE (1:25; clone WM53; catalog 555450, BD Biosciences), CD66b-PerCPCy5.5 (1:100; clone G10F5, catalog 5562254, BD Biosciences), lineage cocktail (LIN, CD3, CD19, CD20, CD56)-APC (1:100; catalog 363601, BD Biosciences), CD80-PE-Cy7 (1:100; clone L307.4; catalog 561135, BD Biosciences), CD86-APC (1:100; clone FUN-1; catalog 560956, BD Biosciences), TLR4-PE (1:100; clone TF901; catalog 564215, BD Biosciences), IgG1-PE (1:200; clone MOPC-21; catalog 554680, BD Biosciences), RAGE-PE (1:500; clone EPR21171; catalog ab237363, Abcam), and IgG-PE (1:500; catalog ab209478, Abcam). To detect ROS production, we applied CellROX Deep Red Reagent (1:500; catalog C10422, Thermo Fisher).

For the detection of phosphoproteins, cells were fixed using Phosflow Fix Buffer I (catalog 557870, BD Biosciences) and permeabilized with Phosflow Perm Buffer III (catalog 558050, BD Biosciences) according to the manufacturer's instructions. Then, the cells were stained with the following mAbs: anti-human p38 MAPK (pT180/pY182)-PE (1:30; clone 36/p38; catalog 562065, BD Biosciences), NFκB (pS529)- PE (1:30; clone K10-895.12.50; catalog 558423, BD Biosciences), and STAT3 (Py705)- PE (1:30; clone 4/P-STAT3; catalog 562072, BD Biosciences). The acquisition was performed using the 10-color flow cytometer BD FACSLyric and FACSuite software (BD Biosciences). Data were analyzed by FlowJo V.10 software (BD Biosciences).

For the isolation of M-MDSC, PBMC from patients with melanoma (n=6) were labeled with anti-human CD33-PE, HLA-DR-V500, CD66b-PerCPCy5.5, and LIN (CD3, CD19, CD20, CD56)-APC mAbs. Monocytes (CD33⁺HLA-DR⁺) and M-MDSC (CD33⁺HLA-DR⁻) were purified using fluorescence-activated cell sorting (FACS), using BD FACSAria IIU cell sorter.

T-cell suppression assay

CD3⁺ T cells were labeled with cell proliferation dye eFluor 450 (10 µM; catalog 65-0842-85, eBioscience) at room temperature for 20 min. Then, T cells were co-cultured with HMGB1- or S100A9-treated monocytes, in vitro generated MDSC or M-MDSC from patients with advanced melanoma in 100 µL L-lysine and L-arginine free RPMI medium for SILAC (88365, Thermo Fisher) supplemented with L-Arginine (150 µM; catalog A5006,

Sigma Aldrich), L-Lysine hydrochloride (0.218 mM; catalog L5626, Sigma Aldrich), 10% heat-inactivated FBS (16140071, Thermo Fisher) and 1% penicillin/streptomycin (15140122, Sigma Aldrich) for 96 hours in 96-well round bottom plates precoated for 2 hours with anti-CD3 (1 μg/mL; clone OKT-3; catalog 16-0037-85, eBioscience) and anti-CD28 antibodies (2 μg/mL; clone CD28.2; catalog IM1376, Beckman Coulter). In some experiments, resatorvid (5 mM) or S100A9 inhibitor tasquinimod (50 uM; catalog HY-10528, MedChemExpress) were added to the co-cultures with in vitro generated MDSC or patient-derived M-MDSC and T cells. Then supernatants were collected, and the proliferation of T cells was assessed by measuring the dilution of proliferation dye eFluor 450 using the BD FACSLyric flow cytometer.

Plasma S100A8/9 and HMGB1 determination
Plasma levels of S100A8/9 and HMGB1 were measured by ELISA kits (DS8900, R&D Systems and NBP2-62766, Novus Biologicals, respectively) according to the manufacturer's instructions. The concentration of S100A8/9 and HMGB1 were checked both in the plasma of patients with advanced melanoma and in the supernatants collected from the co-cultures of T cells with in vitro generated MDSC or patient-derived M-MDSC.

Western blot analysis
Monocytes were washed with ice-cold phosphate-buffered saline and lysed on ice in radioimmuno-precipitation assay buffer (20–199, Sigma Aldrich) supplemented with protease inhibitor (G6521, Promega). Then, cells were centrifuged at 10,000 g for 10 min at 4°C followed by the measurement of the protein concentration in supernatants using Pierce BCA Protein Assay Kit (23225, Thermo Fisher Scientific) and loading 5–10 mg protein per well. Primary antibodies against IDO (rabbit; 1:1,000; catalog D5J4E, Cell Signaling Technology), pSTAT3 (mouse; 1:2,000; 4113S, Cell Signaling Technology), STAT3 (mouse; 1:1,000; catalog 9139S, Cell Signaling Technology), p-p38 (rabbit; 1:1,000; catalog 8690S, Cell Signaling Technology), p38 (rabbit; 1:1,000; catalog 4511S, Cell Signaling Technology), p-p65 (rabbit; 1:1,000; catalog 3033S, Cell Signaling Technology), p-65 (rabbit; 1:1,000; catalog 8242S, Cell Signaling Technology), and GAPDH (rabbit; 1:1,000; catalog 2118S, Cell Signaling Technology) were applied for staining. Protein bands were visualized using SuperSignal West Pico PLUS Chemiluminescent Substrate (catalog 34580, Thermo Fisher) at FUSION-SL-Advance Chemiluminescence reader (PEQLAB Biotechnologie). Quantification of band intensities was performed using ImageJ (NIH).

Microarray analysis
Total RNA was isolated from purified CD14+ human monocytes treated with S100A9 or HMGB1 or non-treated (control) by RNeasy Mini kit (Qiagen) according to the manufacturer's instructions. RNA concentration was determined by the microplate reader Tecan Infinite M200 using a NanoQuant plate. Gene expression analysis was conducted using the Affymetrix Clariom S human assay (Thermo Fisher) following the manufacturer's instructions. A Custom CDF V.25 with ENTREZ-based gene definitions was used to annotate the arrays.[28] The raw fluorescence intensity values were normalized by applying quantile normalization and RMA background correction using an oligo package.[29] Differentially expressed genes were calculated using a limma package.[30] Differences in gene expression with an adjusted p value<0.05 and a logFC>|1| were considered as significant. Gene Set Enrichment Analysis (GSEA) was used to determine whether defined lists of genes exhibit a statistically significant bias in their distribution within a ranked gene list. Pathways belonging to various cell functions were obtained from public databases (KEGG, http://www.genome.jp/kegg and GO, http://geneontology.org/). All statistical procedures and plots were conducted with the R programming language running under the open-source computer software R V.4.3.0.

Single-cell RNA sequencing
10x Genomics Chromium single-cell 3' library was used to prepare the sequencing library. CD14+ monocytes (10³ cells/ mL) were loaded on the chip using the Chromium Single Cell 3' Library, Gel Bead and Multiplex Kit, and Chip Kit (10x Genomics, V.3.1) following the manufacturer's instructions. Subsequent procedures were conducted according to standard manufacturer's protocols. Purified libraries were analyzed using a sequencer NextSeq 550 with 150 bp paired-end reads.

Reads processing and quality control
We used the Seurat R package (V.4.0.1, R V.4.1) to analyze single-cell gene expression data sets.[31] For quality control, genes detected in less than 3 cells and cells with less than 200 genes with non-zero counts were excluded. Cells with a unique feature count of less than 200 and with more than 20% of mitochondrial gene counts were also excluded. The upper limits of feature counts were set to 8,000 for each data set.

Clustering and data visualization
The expression matrices of all samples were merged and data was normalized via SCTransform function of the Seurat V.5 pipeline by regressing out mitochondrial percentage. Samples were integrated using Harmony[32] to correct for batch effects. In the combined data set, 296 cells showed B-cell and T-cell expression patterns and were, therefore, removed from further analysis. After principal component analysis, the top 20 principal components (PCs), a resolution of 0.6 and the harmony reduction were used to identify cell clusters by the FindNeighbors and FindClusters function. Uniform Manifold Approximation and Projection (UMAP) was used for data visualization applying the corrected harmony reduction.
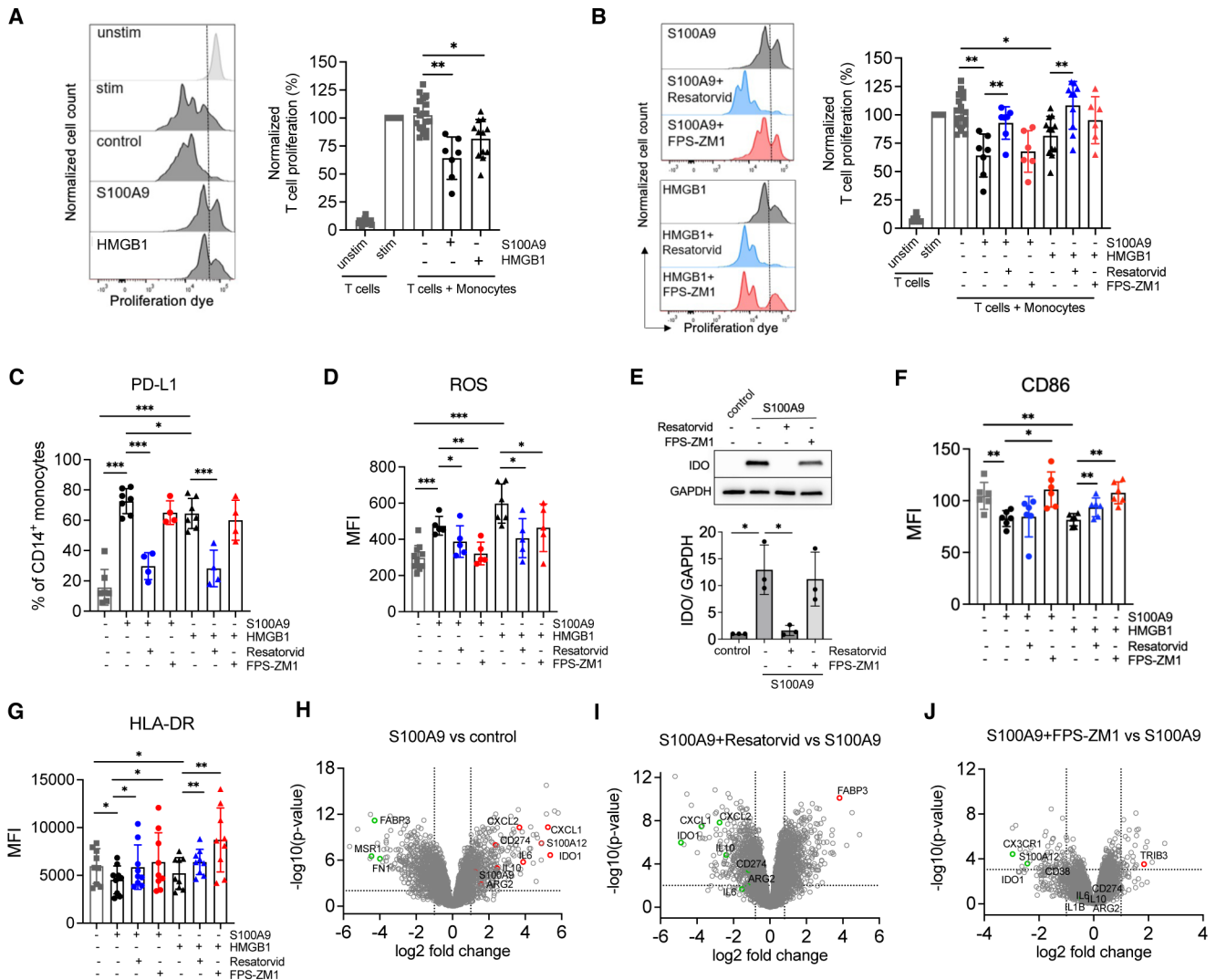
Figure 1 S100A9 and HMGB1 convert monocytes into immunosuppressive MDSC through TLR4 signaling. Monocytes were incubated for 72 hours with S100A9 or HMGB1 (both 5 µg/mL) in the presence of GM-CSF (40 ng/mL). The immunosuppressive capacity of monocytes was determined by flow cytometry after their co-culture for 96 hours with activated CD3+ T cells labeled with the proliferation dye. (A) Representative histograms and cumulative data for T cells cultured for 96 hours alone (unstim), activated with anti-CD3 and anti-CD28 mAbs (stim), or co-cultured with monocytes treated only with GM-CSF or GM-CSF with S100A9 or HMGB1. Results are presented as the percentage of divided T cells normalized to the respective control of stimulated T cells (stim). Mean±SD; n=7–19. (B) In some experiments, monocytes were also pretreated for 1 hour with the TLR4 inhibitor resatorvid (5 µM) or the receptor for advanced glycation endproducts inhibitor FPS-ZM1 (30 nM). Data are presented as the percentage of divided T cells normalized to the respective control. Mean±SD. n=6–19. (C–F) The expression of markers on monocytes was measured by flow cytometry. (C) Results are presented as the percentage of PD-L1+ monocytes among total monocytes. Mean±SD. n=4–7. (D) Data for ROS production are shown as mean fluorescence intensity (MFI). Mean±SD. n=5–11. (E) Expression of IDO-1 in S100A9-treated or HMGB1-treated monocytes pretreated with resatorvid or FPS-ZM1 was measured by western blot. The representative experiment out of three is shown. Quantification of the expression was performed by normalizing the intensities of IDO expression to that of GAPDH. Mean±SD. n=3. Data for (F) CD86 and (G) HLA-DR expression are shown as MFI. Mean±SD. n=6–9. (H–J) Microarray analysis of monocytes cultured for 72 hours with S100A9 or pretreated with resatorvid or FPS-ZM1. Volcano plots showing the differentially expressed genes for (H) S100A9-treated versus control, (I) S100A9+resatorvid versus S100A9-treated, and (J) S100A9+FPS-ZM1 versus S100A9-treated monocytes. Monocytes incubated with GM-CSF only were shown as a control. The horizontal dashed line indicates the significance threshold (p<0.05). Selected differentially expressed genes are shown as red (upregulated) and green circles (downregulated). Vertical dashed line indicates twofold change. n=4. P value was calculated by Mann-Whitney test (A, B). P value was calculated by Wilcoxon test (C, D, F, G). *p<0.05, **p<0.01, ***p<0.001. GM-CSF, granulocyte-macrophage colony-stimulating factor; IDO, indoleamine 2,3-dioxygenase 1; MDSC, myeloid-derived suppressor cells; PD-L1, programmed death-ligand 1; ROS, reactive oxygen species; TLR4, toll like receptor 4.
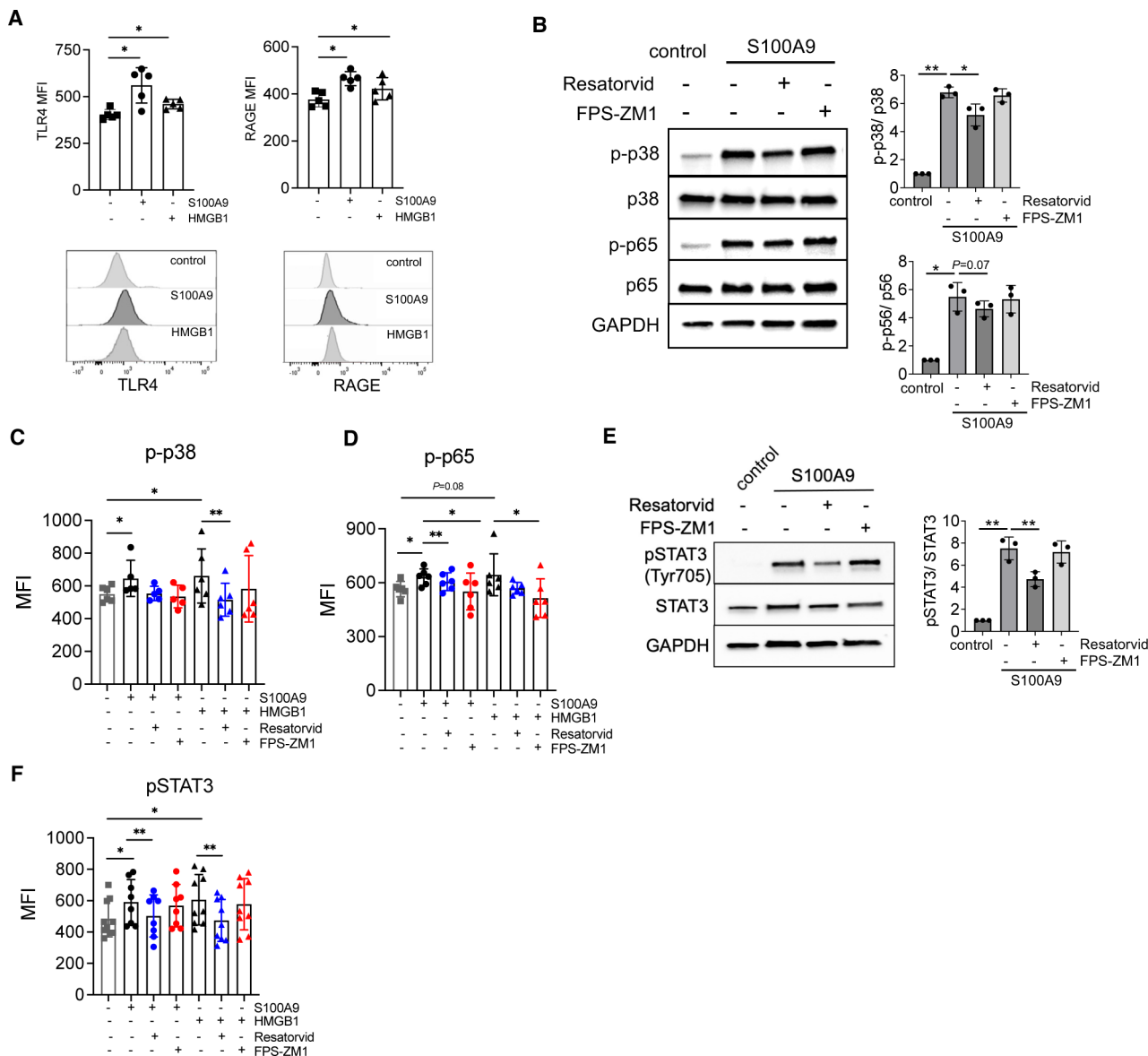
Figure 2 Activation of p38/MAPK, p65/NF-κB, and STAT3 in monocytes induced by S100A9 or HMGB1. (A) Representative histograms and cumulative data for RAGE and TLR4 expression in monocytes treated with HMGB1 or S100A9 for 72 hours and measured by flow cytometry. Results are presented as MFI. Mean±SD. n=5. (B) CD14+ monocytes were incubated with HMGB1 or S100A9 for 1 hour in the presence of resatorvid or FPS-ZM1. Expression of p-p38 and p-p65 were measured by western blot. The representative experiment out of three is shown. Quantification of the expression was performed by normalizing the band intensities of phosphorylated protein to total protein. Mean±SD. n=3. Cumulative data for the expression of (C) p-p38 and (D) p-p65 in monocytes treated with HMGB1 or S100A9 for 72 hours and measured by flow cytometry. Data are presented as MFI. Mean±SD. n=5–6. (E) pSTAT3 expression in monocytes treated with HMGB1 or S100A9 for 24 hours determined by western blot. The representative experiment out of three is shown. Quantification of the expression was performed by normalizing the band intensities of phosphorylated STAT3 to total STAT3. Mean±SD. n=3. (F) Cumulative data for pSTA3 expression in monocytes treated with HMGB1 or S100A9 for 72 hours measured by flow cytometry. Data are depicted as MFI. Mean±SD. n=8–10. P value was calculated by a two-sided paired t-test (A, B, E). P value was calculated by Wilcoxon test (C, D, F). *p<0.05, **p<0.01. MFI, mean fluorescence intensity; RAGE, receptor for advanced glycation endproducts; STAT3, signal transducer and activator of transcription factor 3; TLR4, toll like receptor 4.

Differential gene expression analysis

Differentially expressed genes with respect to different conditions (healthy vs patient monocytes) and to monocyte clusters were identified by FindAllMarkers function of the Seurat V.5 package applying the MAST algorithm with the following criteria: only.pos=false and min. pct=0.2.[33] Selected differentially expressed genes were visualized by VlnPlot() or DoHeatmap() function of the Seurat pipeline. Volcano plots illustrating the distribution of p values and fold changes were generated using the EnhancedVolcano package.[34]
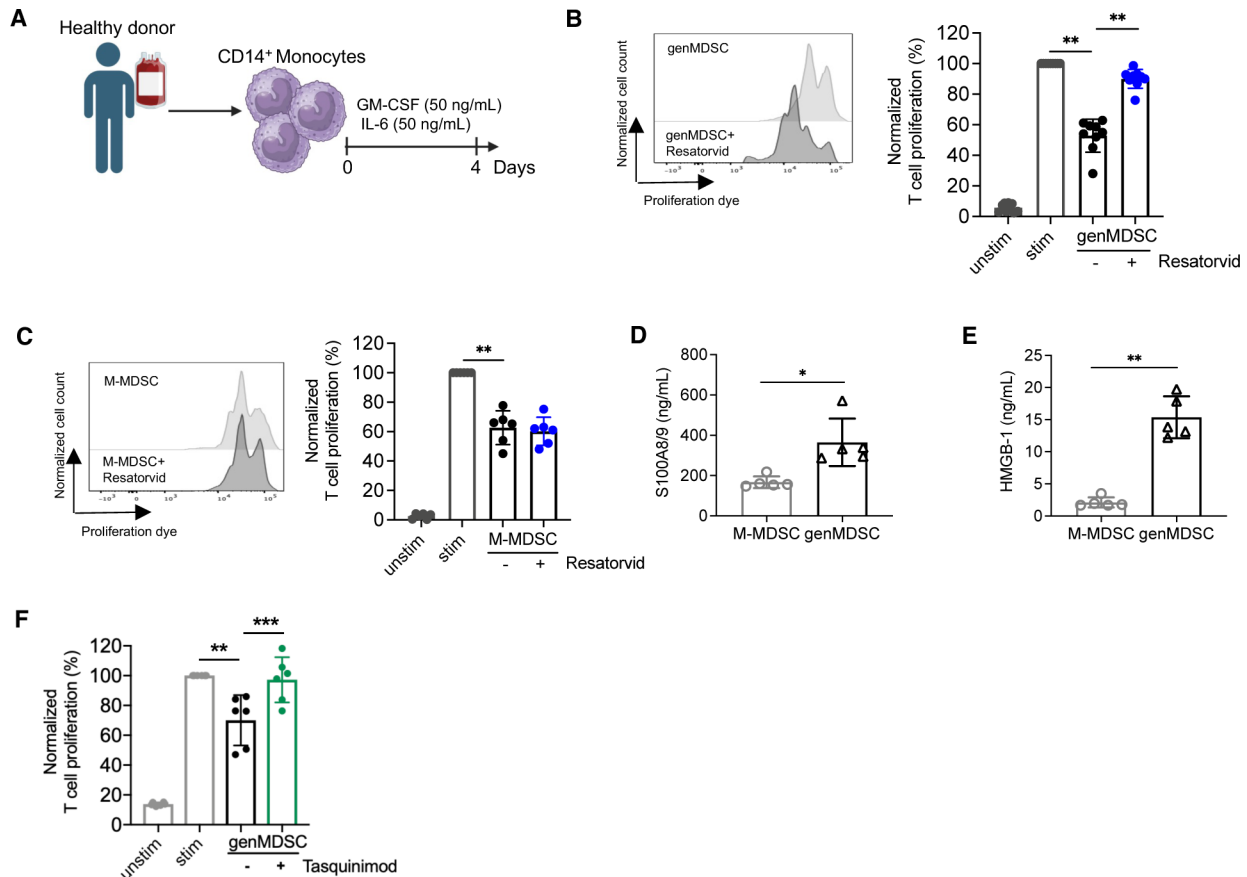
Figure 3 Resatorvid attenuates suppression of T-cell proliferation mediated by in vitro generated MDSC but not patient-derived M-MDSC. (A) Schematic representation of the protocol for human MDSC generation from healthy donor-derived monocytes in vitro. The figure is created with Biorender.com. Activated T cells were co-cultured for 96 hours with (B) generated MDSC (genMDSC) in vitro or with (C) HLA-DR$^{-/low}$ CD33$^+$ M-MDSC from patients with melanoma in the presence or absence of resatorvid. Representative histograms and cumulative data for proliferating T cells are shown as the percentage of divided T cells normalized to the corresponding control of stimulated T-cell control. Mean±SD. n=6–9. Levels of (D) S100A8/9 and (E) HMGB1 in the supernatant from the co-cultures of T cells and genMDSC or patient-derived M-MDSC are shown. Mean±SD. n=5. (F) Activated T cells were co-cultured for 96 hours with genMDSC in the presence or absence of tasquinimod. Cumulative data for proliferating T cells are shown as the percentage of divided T cells normalized to the corresponding control of stimulated T-cell control. Mean±SD. n=6. P value was calculated by Mann-Whitney test (B, C, D, E, F). *p<0.05, **p<0.01. GM-CSF, granulocyte-macrophage colony-stimulating factor; IL, interleukin; M-MDSC, mononuclear-MDSC; MDSC, myeloid-derived suppressor cells.

Pathway enrichment analysis

The clusterProfiler package[35 36] was applied to conduct GSEA using the Reactome database. P value cut-off of 0.05 and correction by Benjamini-Hochberg was applied to the results before visualization in dot plots.

The Cancer Genome Atlas data analysis

RNA sequencing data of patient with metastatic melanoma samples were obtained from the (The Cancer Genome Atlas (TCGA)) database through cBioPortal (http://www.cbioportal.org). The normalized RNA-seq by expectation maximization (RSEM) read counts for the genes of interest were extracted from the TCGA cBioportal.[37] Samples were divided into two groups, the top quartile and the bottom quartile, based on their expression levels of S100A9 or HMGB1. Subsequently, an unpaired Student's t-test was conducted to analyze the difference in mean expression of

MDSC-related markers in the low and high-percentile melanoma samples for the specific gene of interest. The results are presented as a bar plot displaying the genes of interest in y axis and p values in x axis.

Statistical analysis

Statistical analysis was conducted on at least three biological replicates using GraphPad Prism software. Two group comparisons were made using either two-tailed paired Student's t-test or Wilcoxon matched-pairs signed-rank test or Mann-Whitney tests depending on the Gaussian distribution of the data. Correlation analysis was performed using Pearson correlation with a two-tailed p value. PFS curves were generated using the Kaplan-Meier method and statistical comparison was performed by the logrank (Mantel-Cox) test. If a patient showed no sign of tumor progression, data was
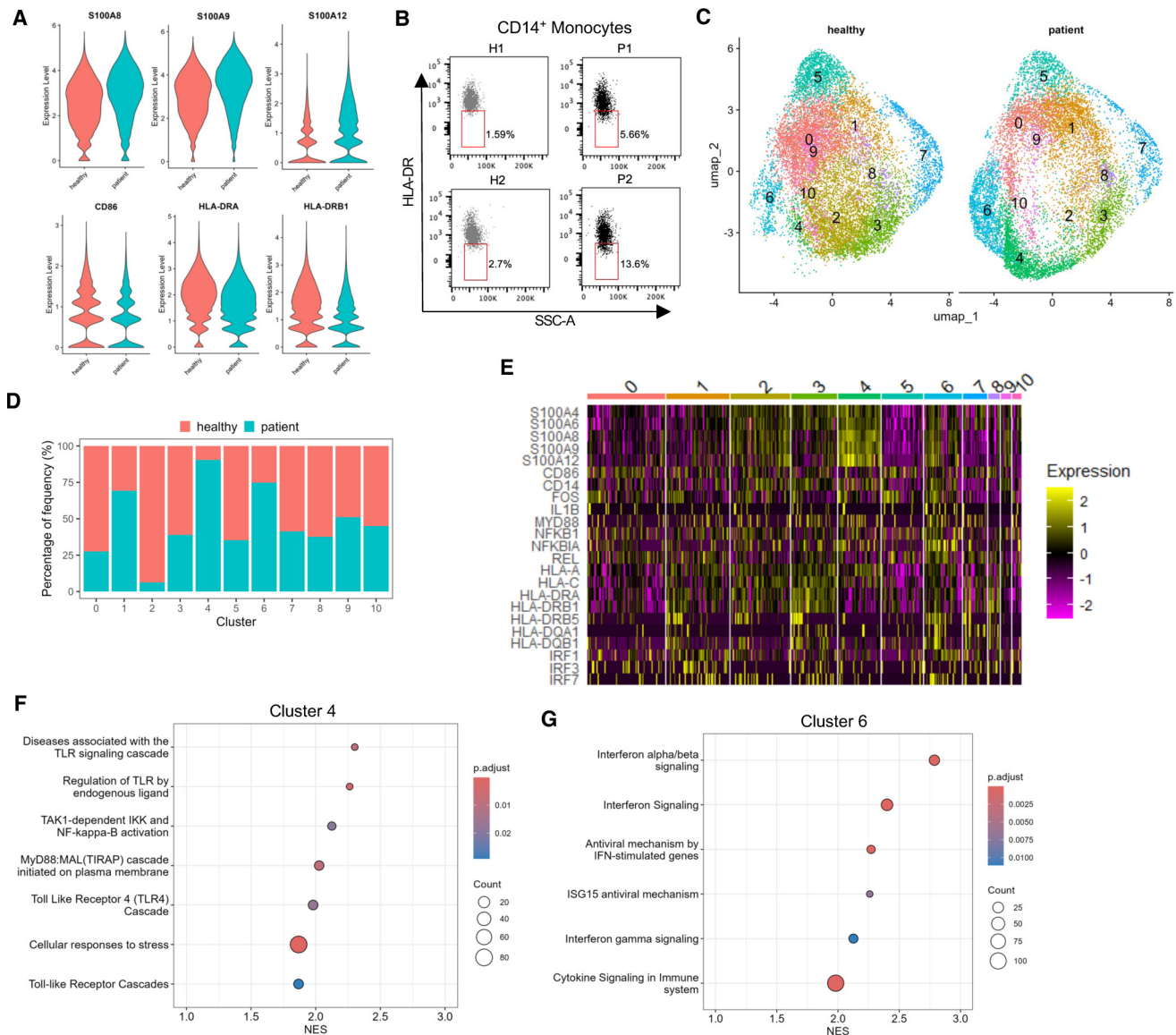
Figure 4 Patient-derived monocytes are enriched in clusters characterized by elevated S100 and reduced major histocompatibility complex class II gene expression. scRNA-seq was performed with circulating CD14+ monocytes derived from patients with advanced melanoma (n=2) and healthy donors (n=2). (A) Violin plots showing the expression level of selected differentially expressed genes (DEGs) (S1008, S100A9, S100A12, CD86, HLA-DRA, HLA-DRB1) in samples from healthy donors and patients with melanoma. (B) HLA-DR expression on CD14+ monocytes from patients with melanoma and healthy donors was measured by flow cytometry. Dot plots showing the frequency of HLA-DR−/low cells among monocytes. (C) UMAP representation of scRNA-seq data for CD14+ monocytes from healthy donors and patients with melanoma.(D) Bar plot showing the frequency of cells from healthy donors or patients for each identified cluster. (E) Heatmap showing the scaled expression of selected DEGs in each cluster. Gene set enrichment of selected Reactome pathways of (F) cluster 4 and (G) cluster 6 were shown. IFN, interferon; scRNA-seq, single-cell RNA sequencing; UMAP, Uniform Manifold Approximation and Projection.

censored regarding the date of last contact. Statistical significance was defined as p<0.05.

RESULTS
S100A9 and HMGB1 converted monocytes into MDSC through TLR4 signaling

We first investigated the immunosuppressive activity of monocytes treated with S100A9 and HMGB1. In addition to their generation from hematopoietic precursors through emergency myelopoiesis, MDSC can also be converted from normal mature myeloid cells within the TME.[38] To mimic TME conditions, healthy donor-derived monocytes were treated with S100A9 and HMGB1 together with GM-CSF.

We found that both S100A9 and HMGB1-treated monocytes inhibited T-cell proliferation (figure 1A). Monocytes incubated with S100A9 showed higher suppression than cells exposed to HMGB1 although these changes were not statistically significant (figure 1A). The TLR4 inhibitor resatorvid (TAK-242)
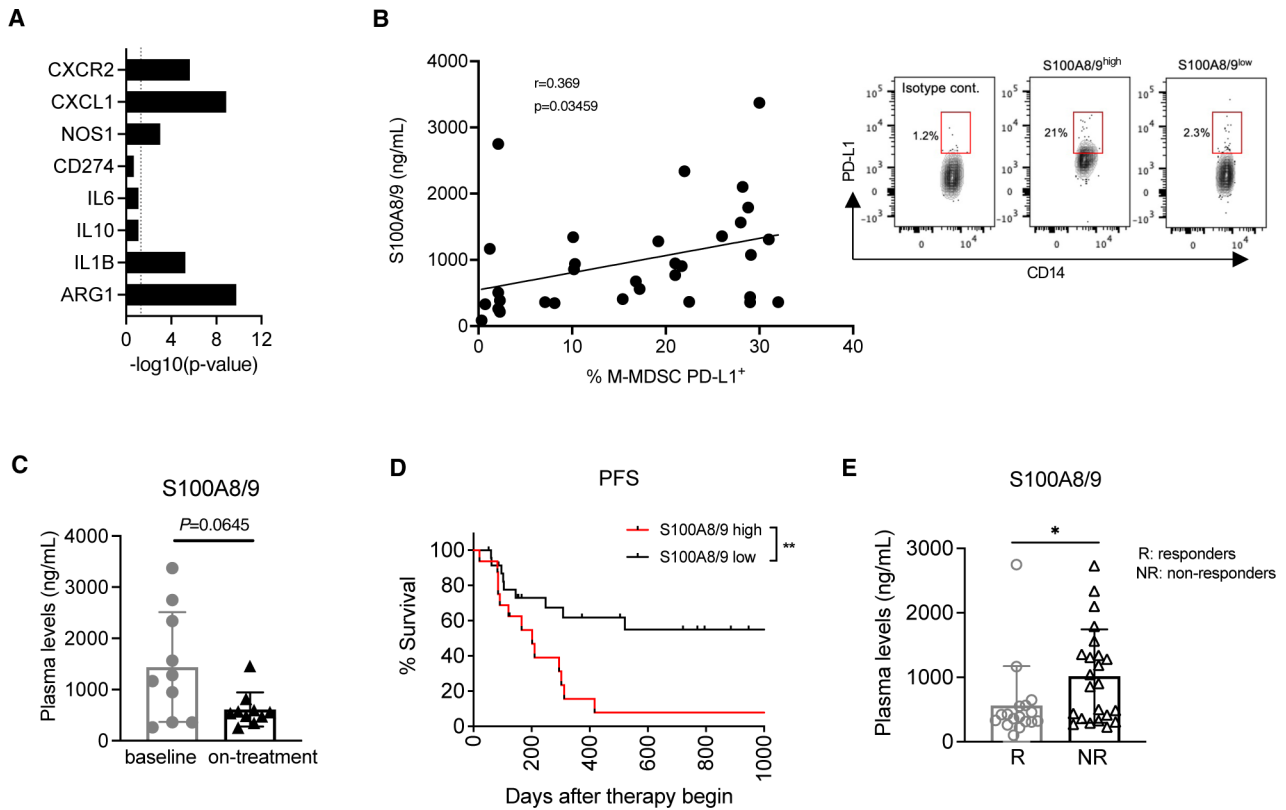
Figure 5 Increased plasma levels of S100A8/9 predict poor PFS in patients with melanoma. (A) The Cancer Genome Atlas analysis of MDSC markers in tumor samples from patients with melanoma stratified into top and bottom 25 percentiles based on S100A9 expression. Differentially upregulated genes in tumors with high S100A9 expression as compared with those in tumors with low S100A9 levels are shown. Dashed vertical line indicates the threshold of statistical significance. n=111. (B–E) The concentration of S100A9 in the plasma of patients with melanoma was measured by ELISA (n=40). The expression of PD-L1 on M-MDSC from these patients was determined by flow cytometry (n=33). (B) The percentage of PD-L1+ M-MDSC among total MDSC was plotted against the plasma levels of S100A8/9 (ng/mL) in patients with melanoma at the baseline (n=33). (C) Plasma levels of S100A8/9 before (baseline) and after first ICI administration (on-treatment) are expressed in ng/mL. Mean±SD. n=10. (D) PFS of patients with melanoma with high (>834.9 ng/mL; n=16) and low (<834.9 ng/mL; n=24) plasma levels of S100A8/9 at the baseline are shown as a Kaplan-Meier curve. (E) Plasma concentrations of S100A8/9 in patients with melanoma responding (R, n=17) and non-responding (NR, n=23) to ICI treatment were expressed in ng/mL. Mean±SD. P value was calculated by Pearson correlation with a two-sided p value (B). P value was calculated by Wilcoxon test (C). P value was calculated by logrank (Mantel-Cox) test (D). P value was calculated by Mann-Whitney test (A, E). *p<0.05, **p<0.01. ARG1, arginase-1; ICI, immune checkpoint inhibitors; IL, interleukin; M-MDSC, mononuclear MDSC; MDSC, myeloid-derived suppressor cells; PD-L1, programmed death-ligand 1; PFS, progression-free survival.

and the RAGE antagonist FPS-ZM1 were employed to block the respective signaling pathways,[26 27] and the concentrations, in which the inhibitors suppress the TLR4 or RAGE signaling in monocytes without exerting cytotoxicity against monocytes and T cells, were determined (online supplemental figure 1A, B). We demonstrated that the pretreatment of monocytes with resatorvid resulted in the reduction of immunosuppression, whereas the exposure to FPS-ZM1 did not alter the ability of monocytes to suppress T-cell proliferation (figure 1B).

We further examined MDSC-related markers on S100A9-treated and HMGB1-treated monocytes. Both ligands induced a strong upregulation of programmed death-ligand 1 (PD-L1) expression and ROS production, which was reversed by the blockade of TLR4 signaling (figure 1C,D). In contrast, the RAGE inhibitor FPS-ZM1 attenuated the increase in

ROS production but not that of PD-L1 expression (figure 1C,D). Moreover, we observed an elevation of IDO-1 expression in monocytes treated with S100A9 that was attenuated by resatorvid, indicating the involvement of TLR4 signaling in the IDO upregulation (figure 1E). In contrast, the treatment with FPS-ZM1 showed only a tendency for the reduction of IDO level that was statistically non-significant (figure 1E). Examining the effect of the monocyte treatment with S100A9 and HMGB1 on CD86 and HLA-DR, we observed a slight but statistically significant decrease in their expression (figure 1F,G). In response to S100A9 treatment, only FPS-ZM1 achieved minimal preservation of CD86 expression. However, both inhibitors were able to slightly keep HLA-DR expression in cells co-cultured with S100A9 (figure 1F,G).

We further conducted a gene expression profiling of monocytes treated with S100A9 since our previous

Table 2 Clinical characteristics of patients with high and low plasma concentrations of S100A8/9

Characteristics	S100A8/9^{high} (>834.9 ng/mL) n=16	S100A8/9^{lows} (<834.9 ng/mL) n=24
Gender, n		
Male	9	9
Female	7	15
Age, n		
≤65 years	8	15
≥65 years	8	9
AJCC Stage, n		
IIIB	2	2
IIIC	3	4
IIID	1	0
IV	10	18
Therapy, n		
Anti-PD-1	5	16
Anti-PD-1/CTLA-4	11	8
Response, n		
Non-responder	11	10
Responder	5	14

AJCC, American Joint Committee on Cancer ; CTLA-4, cytotoxic T-lymphocyte associated protein 4; PD-1, programmed cell death protein-1.

data indicated that S100A9 could induce stronger immunosuppressive activity and higher expression of MDSC-related markers of monocytes than HMGB1. These experiments revealed a significant upregulation of several MDSC-related genes, including *CD274*, *IDO1*, *IL-6*, *IL-10*, arginase 2, *CXCL1*, and *CXCL2* (figure 1H). The expression of *S100A9* and *S100A12* genes was also increased (figure 1H). Co-incubation with resatorvid led to a significant reduction in the expression of these genes, whereas the effect of FPS-ZM1 was much weaker (figure 1I,J). All significantly differentiated genes in each group are provided in online supplemental table 1. Moreover, the analysis revealed the stimulation of several signaling pathways, including JAK-STAT, NF-κB, TLR, and MAPK pathways in S100A9-treated monocytes (online supplemental figure 2A). Although the treatment with both inhibitors downregulated these signaling pathways, resatorvid had a more pronounced effect (online supplemental figure 2B, C), suggesting that the conversion of monocytes into MDSC-like cells by S100A9 and HMGB1 was mainly driven by the TLR4 signaling.

S100A9 or HMGB1 activated p38/MAPK, STAT3 and NF-κB in human monocytes

The expression of both RAGE and TLR4 was enhanced on monocytes incubated with S100A9 or HMGB1, indicating the activation of both signaling pathways (figure 2A). We further investigated the downstream molecules involved in RAGE and TLR4 signaling pathways. Different time points after S100A9 or HMGB1 treatment were chosen to capture phosphorylation of MAPK p38, NF-κB p65 and STAT3 on monocytes and to assess the activation status of monocytes before their co-culture with T cells. Both MAPK p-p38 and NF-κB p-p65 expressions were elevated in monocytes treated with S100A9 (figure 2B–D) or HMGB1 (figure 2C,D). Moreover, the TLR4 inhibitor, but not the RAGE inhibitor, decreased p-p38 expression in monocytes (figure 2B,C). In addition, both inhibitors reduced the intensity of p-NF-κB expression (figure 2B and D).

The signal transducer and activator of transcription factor 3 (STAT3) have been reported to play a pivotal role in MDSC functions.[25] We observed an upregulation of pSTAT3 expression in both S100A9-treated and HMGB1-treated monocytes as compared with the untreated controls (figure 2E,F). The TLR4 inhibitor resatorvid, but not the RAGE inhibitor FPS-ZM1 reduced STAT3 phosphorylation induced by S100A9 or HMGB1 (figure 2E,F), indicating once again that TLR4 signaling is mainly involved in MDSC generation on the treatment of monocytes with S100A9 or HMGB1.

Resatorvid abrogated the immunosuppressive function of in vitro generated MDSC but not that of M-MDSC from patients with melanoma

Given the potential of resatorvid to block the conversion of healthy donor monocytes exposed to S100A9 or HMGB1 into MDSC, we investigated the effect of this inhibitor on the immunosuppressive capacity of generated MDSC, either in vitro as shown in figure 3A or isolated from the peripheral blood of patients with advanced melanoma. In vitro generated (gen)MDSC significantly suppressed T-cell proliferation, and resatorvid led to an attenuation of such effect (figure 3B). However, resatorvid was unable to restore T-cell proliferation suppressed by melanoma patient-derived M-MDSC (figure 3C). We next analyzed the concentrations of the TLR4 ligands S100A8/9 and HMGB1 in the supernatant from T cell and MDSC co-cultures. The supernatants from the co-cultures with genMDSC contained significantly higher levels of S100A8/9 and HMGB1 than those with M-MDSC isolated from patients with melanoma (figure 3D,E). The immunosuppression mediated by genMDSC was significantly reversed by the S100A9 inhibitor tasquinimod, further underscoring the critical role of S100A9 in the genMDSC-mediated effect on T cells (figure 3F).

Patient-derived monocytes show elevated S100 and reduced MHC class II gene expression

To study the transcriptional profiles of circulating CD14$^+$ monocytes in patients with advanced melanoma, we performed scRNA-seq analysis of monocytes isolated from two patients with melanoma without any prior therapy and two healthy donors.

First, we analyzed differentially expressed genes (DEGs) in monocytes from both groups. The results revealed an upregulation of S100 genes (*S100A8, S100A9, S100A12*) in patient monocytes as compared with healthy donor cells (figure 4A). In addition, the expression of NF-κB target genes, including *NFKBIA, NFKB1* and *REL*, was higher in the patient than in the healthy donor group (online supplemental figure 3A). In contrast, MHC II genes such as *HLA-DRA, HLA-DRB1*, and *HLA-DRB5*, as well as the gene encoding the co-stimulatory molecule CD86, showed lower expression in patients than in healthy donors (figure 4A and online supplemental figure 3A). Flow cytometric analysis confirmed decreased HLA-DR expression in CD14$^+$ monocytes from patients with melanoma in comparison with those from healthy donors (figure 4B).

Next, we performed an unsupervised clustering analysis, which revealed 10 monocytic clusters (figure 4C). While clusters 4 and 6 existed predominantly in patient monocytes, cluster 2 consisted mainly of healthy monocytes (figure 4D and online supplemental figure 3B). We performed differential expression analysis on clusters 4 and 6. The top 10 DEGs per cluster are shown in online supplemental figure 3C. The results showed that monocytes from cluster 4 displayed increased expression of *S100* genes, including *S100A4, S100A6, S100A8, S100A9, S100A12* and decreased expression of MHC class II genes, including *HLA-DRB1, HLA-DRB5, HLA-DQB1* (figure 4E and online supplemental figure 3D). Cluster 6 showed high expression of NF-κB target genes such as *NFKBIA,* inflammatory cytokine gene *IL-1B* and genes involved in type 1 interferon (IFN) response such as *IRF7* (figure 4E and online supplemental figure 3E).

The GSEA analysis using Reactome pathways on DEGs, which were identified in clusters 4 and 6, revealed an upregulation of pathways involved in cellular response to stress, NF-κB activation and TLR signaling for cluster 4 and IFN and cytokine signaling for cluster 6 (figure 4F,G). Our findings indicate that monocytes from patients with melanoma display an increased expression of genes associated with NF-κB activation and TLR signaling, as well as increased *S100A8* and *S100A9* gene expression, together with a reduced capacity for antigen presentation as reflected by decreased MHC II gene expression as compared with monocytes from healthy donors.

Increased plasma levels of S100A8/9 predict poor PFS in melanoma

Using the TCGA database, we investigated changes in MDSC-related genes, including *CXCR2, CXCL1, NOS1, CD274, IL-6, IL-10, IL-1B, and ARG1* in tumors from patients with advanced melanoma with high versus low plasma levels of S100A9 or HMGB1. The analysis revealed a notable upregulation of several MDSC-related genes in patients with increased S100A9 concentrations (figure 5A), suggesting a possible link between S100A9 expression and MDSC infiltration in melanoma lesions. In contrast, we did not find such an association in patients with elevated HMGB1 levels (online supplemental figure 4A). Based on these findings, we studied the plasma levels of S100A8/9 and HMGB1 in the cohort of patients with metastatic melanoma prior to the initiation of ICI treatment. A positive correlation was observed between an elevated plasma level of S100A8/9 and an increased frequency of circulating M-MDSC expressing PD-L1 (figure 5B). However, we failed to observe a similar correlation between PD-L1$^+$ M-MDSC and HMGB1 (online supplemental figure 4B).

Next, we studied plasma levels of S100A8/9 in patients with melanoma receiving ICI therapy (table 2). We demonstrated a tendency for the reduction of this molecule 1 month after the first ICI administration as compared with the basal levels (figure 5C). Furthermore, to distribute patients in the groups with low and high concentrations of S100A8/A9 and HMGB1 in plasma, we used their median values (834.9 and 55.37 ng/mL, respectively) as a cut-off. ICI-treated patients with high S100A8/A9 concentrations displayed a significantly shorter PFS than those with low levels (figure 5D). In addition, the patients responding to the ICI immunotherapy displayed significantly lower plasma levels of S100A8/9 at the baseline (figure 5E). In contrast, similar associations were not found for HMGB1 plasma levels (online supplemental figure 4C, D). Collectively, these results suggest an association between the programmed cell death protein-1 (PD-1) blockade immunotherapy and plasma S100A8/9 levels in patients with advanced melanoma, underscoring the potential of this factor as a prognostic biomarker in melanoma.

DISCUSSION

We showed that exposure of healthy donor-derived CD14$^+$ monocytes to alarmins S100A9 and HMGB1 results in their acquisition of MDSC-like properties, as reflected by their ability to inhibit T-cell proliferation. Analyzing the mechanisms of such monocyte conversion into MDSC, we found an upregulation of PD-L1 expression, which is present in MDSC and induces T-cell exhaustion through interaction with PD-1.[5] Earlier, we demonstrated that both melanoma-derived extracellular vesicles[39] and soluble HSP90α protein[40] induce the upregulation of PD-L1 on healthy monocytes, in a manner dependent on TLR4 signaling. Moreover, monocytes treated with S100A8/9 and HMGB1 showed decreased expression of HLA-DR and CD86 at both protein and messenger RNA (mRNA) levels. MDSC typically exhibit low expression of these molecules, resulting in reduced antigen presentation and inhibition of T-cell functions.[41]

RAGE and TLR4 triggering with S100A9 and HMGB1 were previously reported to activate multiple factors, including MAPK, STAT3 and NF-κB, that promoted the secretion of various inflammatory mediators and the production of ROS.[22] In agreement with these findings, we found that both alarmins increased the expression of p-p38 MAPK, p-STAT3 and p-p65 NF-κB as well as stimulated ROS production in monocytes. Furthermore, S100A9 upregulated the expression of *IL-6, IL-10, IDO1, S100A9*, and *S100A12* at the mRNA level.

After the treatment with S100A9 or HMGB1, we observed an increased expression of both TLR4 and RAGE at the protein level, which is in agreement with the previous study, showing that NF-κB activation via TLR4 or RAGE signaling leads to the upregulation of RAGE or TLR4 expression.[42]

A study using RAGE-deficient mice demonstrated that RAGE signaling promote the accumulation and immunosuppressive function of MDSC.[43] We observed that the treatment of monocytes with HMGB1 and S100A9 led to the acquisition of an MDSC-like phenotype, primarily via TLR4 signaling pathways, suggesting a less important role for RAGE in this context. This finding aligns with reports indicating a higher affinity of HMGB1 for TLR4 than for RAGE.[44 45] Furthermore, S100A8/9 was shown to induce TLR4-dependent expansion of megakaryocytes that promoted the progression of multiple myeloma in mice.[46] Interestingly, the TLR4 adaptor proteins MyD88 and TIRAP were found to interact with phosphorylated RAGE, suggesting a potential crosstalk between the two receptor pathways.[47] Additionally, TLR4 knockout mice were reported to exhibit diminished RAGE expression.[48] These observations may suggest a possible bidirectional interaction between RAGE and TLR4 receptors.

Our results demonstrated that the TLR4 inhibitor resatorvid was more effective in inhibiting S100A9 and HMGB1-induced conversion of normal monocytes into MDSC-like cells than the RAGE inhibitor FPS-ZM1. It is plausible that resatorvid could also block RAGE signaling since it was shown that TLR4 signaling is acting downstream of RAGE signaling.[49] Resatorvid reversed the suppression of T-cell proliferation by in vitro generated MDSC, likely due to the elevated levels of S100A9 and HMGB1 detected in the supernatant of their co-culture with T cells as compared with that in T cell-M-MDSC co-cultures. Furthermore, the inhibition of S100A9 by tasquinimod blocked genMDSC-mediated suppression of T-cell proliferation, highlighting thereby a pivotal role of S100A9 in this immunosuppression. It is possible that in vitro generated MDSC, being in an early transformation state, can be more susceptible to TLR4 inhibition than melanoma patient-derived circulating M-MDSC, which have an established immunosuppressive activity. Thus, inhibiting TLR4 signaling or targeting directly S100A9 may be more effective in myeloid cells at the beginning of their transformation into MDSC. However, it should be noted that inhibiting TLR4 may dampen immune responses against infection.[50] However, targeting S100A9 might be a more promising approach than TLR4 inhibition. Preclinical studies in mouse models of prostate cancer and melanoma demonstrated the role of tasquinimod in inhibiting the functions of MDSC.[51] This S100A9 inhibitor was studied in metastatic castration-resistant prostate cancer in the frame of phase II and III clinical trials that revealed a survival improvement in patients with prostate cancer.[52] Although phase II trials of tasquinimod showed promising results in terms of PFS,[53] phase III trials failed to result in an overall survival benefit.[52] Tasquinimod is currently testing in a phase Ib/IIa clinical trial in patients with multiple myeloma (NCT04405167). Hence, strategies involving the targeting of S100A9 should be explored in the context of melanoma immunotherapy.

Patient-specific clusters found in our sc-RNAseq analysis of circulating CD14+ monocytes were characterized by an increased expression of genes involved in NF-κB signaling and reduced MHC II gene expression. Such changes were described in the literature as typical for myeloid cells with immunosuppressive functions.[54 55] Thus, these clusters could identify monocytes with immunosuppressive functions in the peripheral blood of patients with melanoma. In addition, we showed increased *S100A9* gene expression in patient monocytes as compared with healthy monocytes. In agreement with this finding, increased S100A9 expression has recently been demonstrated in monocytes from patients with melanoma who did not respond to anti-PD-1 antibody immunotherapy.[56]

It has been reported that elevated levels of HMGB1 in the TME and the peripheral blood of patients with various tumors, including melanoma, correlate with the disease progression and worse overall patient survival.[57] However, we found no association between the plasma HMGB1 levels and the clinical outcome of patients with melanoma.

Although we found very low plasma concentrations of S100A9 (<10 pg/mL) in patients with melanoma (data not shown), we observed a significant amount of S100A8/9 heterodimer in the plasma. This might be due to a higher abundance and stability of the heterodimer in circulation as compared with homodimers S100A8 and S100A9.[58 59] Moreover, increased plasma S100A8/9 levels in ICI-treated patients correlated with their shorter PFS. Responders had significantly lower plasma levels of S100A8/9 at baseline. Our data are consistent with previous studies, showing that elevated levels of circulating S100A8/9 correlate with the disease progression in different cancer entities.[15 20 21] In addition, we previously reported the correlation between elevated serum levels of S100A8/A9 and reduced PFS in patients with melanoma treated with pembrolizumab.[60]

Differences in biological activities between the S100A8/9 heterodimer and the S100A9 monomer have been reported.[58 59 61] Our in vitro experiments demonstrated that S100A9 could induce MDSC-like properties in monocytes, and expression of S100A9 is upregulated in monocytes from patients with melanoma. Furthermore, TCGA data showed that S100A9 expression correlated with

MDSC-related markers in tumor tissues, suggesting a significant role for S100A9 in MDSC-mediated immunosuppression and highlighting its potential as an immunotherapeutic target. In addition, our findings indicated that plasma levels of the S100A8/9 heterodimer could serve as a biomarker, correlating with the PFS of patients with melanoma.

Taken together, our findings demonstrated an important role of TLR4 and, to a lesser extent, RAGE signaling pathways in the conversion of healthy donor-derived circulating monocytes into immunosuppressive MDSC-like cells. This suggests the possibility of targeting TLR4, and in particular S100A9, to prevent such conversion. Furthermore, we showed that elevated plasma S100A8/A9 levels in patients with melanoma could be used as a biomarker to predict the accumulation of immunosuppressive monocytes and to assess the efficacy of ICI therapy in these patients.

Author affiliations
[1]Skin Cancer Unit, German Cancer Research Center, Heidelberg, Germany
[2]Department of Dermatology Venereology and Allergology, University Medical Centre Mannheim, Heidelberg University, Mannheim, Germany
[3]DKFZ-Hector Cancer Institute at the University Medical Center Mannheim, Mannheim, Germany
[4]Mannheim Institute for Innate Immunoscience (MI3), Medical Faculty Mannheim, Heidelberg University, Mannheim, Germany
[5]Department of Immunobiochemistry, Mannheim Institute for Innate Immunoscience (MI3), Medical Faculty Mannheim, Heidelberg University, Mannheim, Germany
[6]NGS Core Facility, Medical Faculty Mannheim, Heidelberg University, Mannheim, Germany

ORCID iDs
Feyza Gül Özbay Kurt http://orcid.org/0000-0003-4086-6469
Viktor Umansky http://orcid.org/0000-0003-0259-1839

REFERENCES

1. Schadendorf D, van Akkooi ACJ, Berking C, *et al*. Melanoma. *Lancet* 2018;392:971–84.
2. Petrova V, Arkhypov I, Weber R, *et al*. Modern Aspects of Immunotherapy with Checkpoint Inhibitors in Melanoma. *Int J Mol Sci* 2020;21:2367.
3. Weide B, Martens A, Zelba H, *et al*. Myeloid-derived suppressor cells predict survival of patients with advanced melanoma: comparison with regulatory T cells and NY-ESO-1- or melan-A-specific T cells. *Clin Cancer Res* 2014;20:1601–9.
4. Cassetta L, Bruderek K, Skrzeczynska-Moncznik J, *et al*. Differential expansion of circulating human MDSC subsets in patients with cancer, infection and inflammation. *J Immunother Cancer* 2020;8:e001223.
5. Groth C, Hu X, Weber R, *et al*. Immunosuppression mediated by myeloid-derived suppressor cells (MDSCs) during tumour progression. *Br J Cancer* 2019;120:16–25.
6. Ostrand-Rosenberg S, Sinha P. Myeloid-derived suppressor cells: linking inflammation and cancer. *J Immunol* 2009;182:4499–506.
7. Ozbay Kurt FG, Lasser S, Arkhypov I, *et al*. Enhancing immunotherapy response in melanoma: myeloid-derived suppressor cells as a therapeutic target. *J Clin Invest* 2023;133:e170762.
8. Siret C, Collignon A, Silvy F, *et al*. Deciphering the Crosstalk Between Myeloid-Derived Suppressor Cells and Regulatory T Cells in Pancreatic Ductal Adenocarcinoma. *Front Immunol* 2019;10:3070.
9. Marvel D, Gabrilovich DI. Myeloid-derived suppressor cells in the tumor microenvironment: expect the unexpected. *J Clin Invest* 2015;125:3356–64.
10. Kanterman J, Sade-Feldman M, Baniyash M. New insights into chronic inflammation-induced immunosuppression. *Semin Cancer Biol* 2012;22:307–18.
11. Zhao H, Wu L, Yan G, *et al*. Inflammation and tumor progression: signaling pathways and targeted intervention. *Signal Transduct Target Ther* 2021;6:263.
12. Umansky V, Sevko A, Gebhardt C, *et al*. Myeloid-derived suppressor cells in malignant melanoma. *J Dtsch Dermatol Ges* 2014;12:1021–7.
13. Sinha P, Okoro C, Foell D, *et al*. Proinflammatory S100 proteins regulate the accumulation of myeloid-derived suppressor cells. *J Immunol* 2008;181:4666–75.
14. Jin S, Yang Z, Hao X, *et al*. Roles of HMGB1 in regulating myeloid-derived suppressor cells in the tumor microenvironment. *Biomark Res* 2020;8:21.
15. Srikrishna G. S100A8 and S100A9: new insights into their roles in malignancy. *J Innate Immun* 2012;4:31–40.
16. Xia P, Ji X, Yan L, *et al*. Roles of S100A8, S100A9 and S100A12 in infection, inflammation and immunity. *Immunology* 2024;171:365–76.
17. Vogl T, Gharibyan AL, Morozova-Roche LA. Pro-inflammatory S100A8 and S100A9 proteins: self-assembly into multifunctional native and amyloid complexes. *Int J Mol Sci* 2012;13:2893–917.
18. Wang S, Song R, Wang Z, *et al*. S100A8/A9 in Inflammation. *Front Immunol* 2018;9:1298.

19 Chen R, Kang R, Tang D. The mechanism of HMGB1 secretion and release. *Exp Mol Med* 2022;54:91–102.

20 Tang D, Kang R, Zeh HJ, *et al*. The multifunctional protein HMGB1: 50 years of discovery. *Nat Rev Immunol* 2023;23:824–41.

21 Wu T, Zhang W, Yang G, *et al*. HMGB1 overexpression as a prognostic factor for survival in cancer: a meta-analysis and systematic review. *Oncotarget* 2016;7:50417–27.

22 Ostrand-Rosenberg S, Huecksteadt T, Sanders K. The Receptor for Advanced Glycation Endproducts (RAGE) and Its Ligands S100A8/A9 and High Mobility Group Box Protein 1 (HMGB1) Are Key Regulators of Myeloid-Derived Suppressor Cells. *Cancers (Basel)* 2023;15:1026.

23 Zhou H, Zhao C, Shao R, *et al*. The functions and regulatory pathways of S100A8/A9 and its receptors in cancers. *Front Pharmacol* 2023;14:1187741.

24 Huang M, Wu R, Chen L, *et al*. S100A9 Regulates MDSCs-Mediated Immune Suppression via the RAGE and TLR4 Signaling Pathways in Colorectal Carcinoma. *Front Immunol* 2019;10:2243.

25 Veglia F, Sanseviero E, Gabrilovich DI. Myeloid-derived suppressor cells in the era of increasing myeloid cell diversity. *Nat Rev Immunol* 2021;21:485–98.

26 Matsunaga N, Tsuchimori N, Matsumoto T, *et al*. TAK-242 (resatorvid), a small-molecule inhibitor of Toll-like receptor (TLR) 4 signaling, binds selectively to TLR4 and interferes with interactions between TLR4 and its adaptor molecules. *Mol Pharmacol* 2011;79:34–41.

27 Deane R, Singh I, Sagare AP, *et al*. A multimodal RAGE-specific inhibitor reduces amyloid β-mediated brain disorder in A mouse model of Alzheimer disease. *J Clin Invest* 2012;122:1377–92.

28 Dai M, Wang P, Boyd AD, *et al*. Evolving gene/transcript definitions significantly alter the interpretation of GeneChip data. *Nucleic Acids Res* 2005;33:e175.

29 Carvalho BS, Irizarry RA. A framework for oligonucleotide microarray preprocessing. *Bioinformatics* 2010;26:2363–7.

30 Ritchie ME, Phipson B, Wu D, *et al*. limma powers differential expression analyses for RNA-sequencing and microarray studies. *Nucleic Acids Res* 2015;43:e47.

31 Stuart T, Butler A, Hoffman P, *et al*. Comprehensive Integration of Single-Cell Data. *Cell* 2019;177:1888–902.

32 Korsunsky I, Millard N, Fan J, *et al*. Fast, sensitive and accurate integration of single-cell data with Harmony. *Nat Methods* 2019;16:1289–96.

33 Finak G, McDavid A, Yajima M, *et al*. MAST: a flexible statistical framework for assessing transcriptional changes and characterizing heterogeneity in single-cell RNA sequencing data. *Genome Biol* 2015;16:278.

34 Blighe K, Rana S, Lewis M. EnhancedVolcano: publication-ready volcano plots with enhanced colouring and labeling. R package version 1200. 2023. Available: https://bioconductororg/packages/EnhancedVolcano

35 Wu T, Hu E, Xu S, *et al*. clusterProfiler 4.0: A universal enrichment tool for interpreting omics data. *Innovation (Camb)* 2021;2:100141.

36 Yu G, Wang L-G, Han Y, *et al*. clusterProfiler: an R package for comparing biological themes among gene clusters. *OMICS* 2012;16:284–7.

37 Van Allen EM, Miao D, Schilling B, *et al*. Genomic correlates of response to CTLA-4 blockade in metastatic melanoma. *Science* 2015;350:207–11.

38 Huber V, Vallacchi V, Fleming V, *et al*. Tumor-derived microRNAs induce myeloid suppressor cells and predict immunotherapy resistance in melanoma. *J Clin Invest* 2018;128:5505–16.

39 Fleming V, Hu X, Weller C, *et al*. Melanoma Extracellular Vesicles Generate Immunosuppressive Myeloid Cells by Upregulating PD-L1 via TLR4 Signaling. *Cancer Res* 2019;79:4715–28.

40 Arkhypov I, Özbay Kurt FG, Bitsch R, *et al*. HSP90α induces immunosuppressive myeloid cells in melanoma via TLR4 signaling. *J Immunother Cancer* 2022;10:e005551.

41 Gabrilovich DI. Myeloid-Derived Suppressor Cells. *Cancer Immunol Res* 2017;5:3–8.

42 Wang L, Wu J, Guo X, *et al*. RAGE Plays a Role in LPS-Induced NF-κB Activation and Endothelial Hyperpermeability. *Sensors (Basel)* 2017;17:722.

43 Wuren T, Huecksteadt T, Beck E, *et al*. The receptor for advanced glycation endproducts (RAGE) decreases survival of tumor-bearing mice by enhancing the generation of lung metastasis-associated myeloid-derived suppressor cells. *Cell Immunol* 2021;365:104379.

44 He M, Bianchi ME, Coleman TR, *et al*. Exploring the biological functional mechanism of the HMGB1/TLR4/MD-2 complex by surface plasmon resonance. *Mol Med* 2018;24:21.

45 Ling Y, Yang Z-Y, Yin T, *et al*. Heparin changes the conformation of high-mobility group protein 1 and decreases its affinity toward receptor for advanced glycation endproducts in vitro. *Int Immunopharmacol* 2011;11:187–93.

46 Lin C, Garcia-Gerique L, Bonner EE, *et al*. S100A8/S100A9 Promote Progression of Multiple Myeloma via Expansion of Megakaryocytes. *Cancer Res Commun* 2023;3:420–30.

47 Sakaguchi M, Murata H, Yamamoto K, *et al*. TIRAP, an adaptor protein for TLR2/4, transduces a signal from RAGE phosphorylated upon ligand binding. *PLoS One* 2011;6:e23132.

48 Zhong H, Li X, Zhou S, *et al*. Interplay between RAGE and TLR4 Regulates HMGB1-Induced Inflammation by Promoting Cell Surface Expression of RAGE and TLR4. *J Immunol* 2020;205:767–75.

49 Yan L, Li Y, Tan T, *et al*. RAGE-TLR4 Crosstalk Is the Key Mechanism by Which High Glucose Enhances the Lipopolysaccharide-Induced Inflammatory Response in Primary Bovine Alveolar Macrophages. *Int J Mol Sci* 2023;24:7007.

50 Duan T, Du Y, Xing C, *et al*. Toll-Like Receptor Signaling and Its Role in Cell-Mediated Immunity. *Front Immunol* 2022;13:812774.

51 Shen L, Sundstedt A, Ciesielski M, *et al*. Tasquinimod modulates suppressive myeloid cells and enhances cancer immunotherapies in murine models. *Cancer Immunol Res* 2015;3:136–48.

52 Mehta AR, Armstrong AJ. Tasquinimod in the treatment of castrate-resistant prostate cancer - current status and future prospects. *Ther Adv Urol* 2016;8:9–18.

53 Pili R, Häggman M, Stadler WM, *et al*. Phase II randomized, double-blind, placebo-controlled study of tasquinimod in men with minimally symptomatic metastatic castrate-resistant prostate cancer. *J Clin Oncol* 2011;29:4022–8.

54 Li K, Shi H, Zhang B, *et al*. Myeloid-derived suppressor cells as immunosuppressive regulators and therapeutic targets in cancer. *Signal Transduct Target Ther* 2021;6:362.

55 Biswas SK, Lewis CE. NF-κB as a central regulator of macrophage function in tumors. *J Leukoc Biol* 2010;88:877–84.

56 Rad Pour S, Pico de Coaña Y, Demorentin XM, *et al*. Predicting anti-PD-1 responders in malignant melanoma from the frequency of S100A9+ monocytes in the blood. *J Immunother Cancer* 2021;9:e002171.

57 Li Q, Li J, Wen T, *et al*. Overexpression of HMGB1 in melanoma predicts patient survival and suppression of HMGB1 induces cell cycle arrest and senescence in association with p21 (Waf1/Cip1) up-regulation via a p53-independent, Sp1-dependent pathway. *Oncotarget* 2014;5:6387–403.

58 Riva M, He Z, Källberg E, *et al*. Human S100A9 protein is stabilized by inflammatory stimuli via the formation of proteolytically-resistant homodimers. *PLoS One* 2013;8:e61832.

59 Real F, Zhu A, Huang B, *et al*. S100A8-mediated metabolic adaptation controls HIV-1 persistence in macrophages in vivo. *Nat Commun* 2022;13:5956.

60 Wagner NB, Weide B, Gries M, *et al*. Tumor microenvironment-derived S100A8/A9 is a novel prognostic biomarker for advanced melanoma patients and during immunotherapy with anti-PD-1 antibodies. *J Immunother Cancer* 2019;7:343.

61 Vogl T, Stratis A, Wixler V, *et al*. Autoinhibitory regulation of S100A8/S100A9 alarmin activity locally restricts sterile inflammation. *J Clin Invest* 2018;128:1852–66.